

Structural Analysis of Aerostat Flexible Structure by the Finite-Element Method

John D. Hunt*

TCOM Corporation, Columbia, Md.

TCOM aerostats have been analyzed to investigate the stresses, deflections, and potential for buckling of the hull, empennage, and suspension system under various configurations and loading conditions. The finite-element structural analysis shows the material strength requirements, minimum pressure differential requirements, and areas where material can be optimized in strength and weight. Graphic output from the analysis shows the deformed shapes and the stress distributions. The results of the analysis show the hull material and internal pressures used to optimum. The empennage can use lower strength materials for weight reduction.

Introduction

WITH the development of stronger tethers, a structural analysis was required to determine if the aerostat structure strength is matched to the tether. A finite-element analysis was performed to determine the structural behavior of the aerostat under various loading conditions.

This article describes the method of analysis, the analysis model, the applied loads, and the typical results for 250 (250,000 ft³) and 365 aerostats.

Method

The analysis is performed using NASTRAN,[†] a large finite-element computer program for static and dynamic structural analysis. The distributed physical properties of the aerostat are represented by a model consisting of finite elements or substructures which are interconnected at a finite number of grid points, to which loads are applied. All data pertain to this idealized structural model.

The model is made up of grid points interconnected by structural elements such as bars or plates. Constraints are applied to various grid points to define fixed points and to specify boundary conditions. Based on the properties of the elements, stiffness matrix K is generated. Loads are applied as concentrated forces on grid points or as distributed loads or pressures on elements.

The governing equation for static problems is

$$\{U\} = [K]^{-1} \{P\} \quad (1)$$

where P is a vector of loads applied to the grid points, and U is an unknown vector of grid point displacements. The element internal forces or stresses are then calculated from the grid point displacements and the physical properties of the elements.

Description of the Model

The model is not fine enough to give detailed stress concentration results but gives overall stress patterns. The grid points on the hull are generally located on gore seals and spaced so as to form nearly square quadrilateral elements or nearly equilateral triangular elements. At the load patches, the points are located at the ends of the patches. Grid points on the fins are located on ribs and at the same span distance as the guy lines.

The confluence point is the fixed grid point of the model. The suspension system is simplified to rods from the ends of each load patch to the confluence point. Guy lines are connected between the horizontal and lower vertical fins only. The upper fin guys are not loaded for the condition of helium in the fins and aerodynamic loads with positive angles of attack. As all empennage grid points are located on ribs, the guy lines on the model are connected to adjacent ribs instead of between ribs.

Undeformed shape plots of the 250 and 365 aerostat models are shown in Fig. 1. The 365 aerostat is similar to the 250 aerostat except that a cylindrical section is added at the point of maximum diameter. Some elements such as fin ribs are not shown in this figure for clarity.

Only one side of the aerostat is modeled because of symmetry and in order to reduce the size and cost of the analysis. Displacements and forces are considered only in the longitudinal, X , and vertical, Z , directions. All boundary points are constrained so as to remain in the X - Z plane.

Material Properties

Material properties, such as elastic modulus and density, are generally obtained from the tests. Physical properties of the elements such as thickness, area, and moment of inertia are given dimensions of unity. The material properties are then in terms of the elastic modulus times the area, thickness, etc.

Hull and Fin Laminate

The elastic properties of the hull and fin material were obtained by biaxial stress cylinder tests performed by the aerostat manufacturer.¹ The coefficients for this anisotropic material are used in the following expression relating stress to strain:

$$\begin{Bmatrix} \sigma_x \\ \sigma_y \\ \sigma_{xy} \end{Bmatrix} = \begin{bmatrix} C_{11} & C_{12} & C_{13} \\ C_{21} & C_{22} & C_{23} \\ C_{31} & C_{32} & C_{33} \end{bmatrix} \begin{Bmatrix} \epsilon_x \\ \epsilon_y \\ \gamma_{xy} \end{Bmatrix} \quad (2)$$

(Stress) (Elastic coefficients) (Strain)

The elastic coefficients for the material membrane properties in units of lb/ft are

$$[C_{ij}] = \begin{bmatrix} 32,400 & 8,880 & 0 \\ 8,880 & 27,000 & 0 \\ 0 & 0 & 2,040 \end{bmatrix} \quad (3)$$

Presented as Paper 81-1342 at the AIAA Lighter-than-Air Conference, Annapolis, Md., July 8-10, 1981; submitted July 21, 1981; revision received Oct. 23, 1981. Copyright © American Institute of Aeronautics and Astronautics, Inc., 1981. All rights reserved.

*Senior Engineer, Aerostat Systems Department.

†MSC/NASTRAN—maintained by The MacNeal-Schwendler Corp., Los Angeles, Calif.

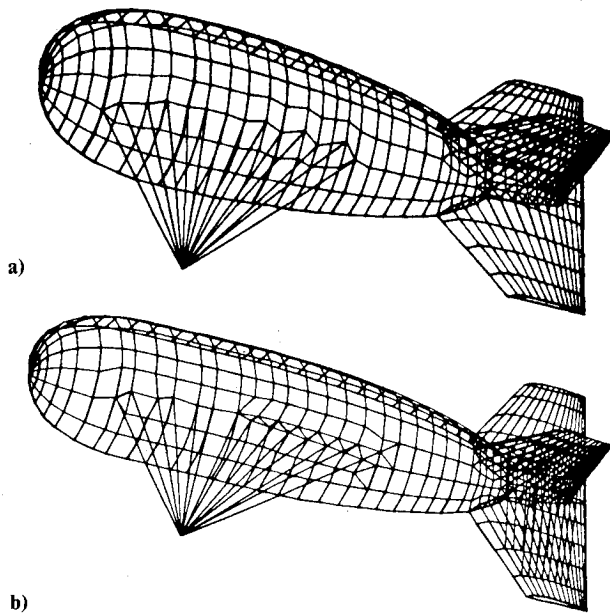


Fig. 1 Analysis model: a) 250 aerostat; b) 365 aerostat.

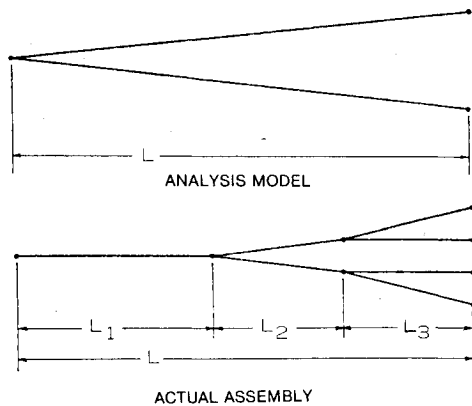


Fig. 2 Suspension line.

The density times thickness, ρT , is 0.055 lb/ft^2 . In the area of the ballonnet, the ρT was increased by 0.050 lb/ft^2 and, in the area of the ballonnet end caps, by 0.100 lb/ft^2 in order to account for the ballonnet weight.

A cylindrical structure built of membrane elements is not stable, in the same way a ring built of truss elements is not stable. A very small amount of bending stiffness (500 ft-lb/rad-ft) was added to the hull and fin material in order to stabilize the structure. The bending moments introduced are very small in comparison to the membrane loads—typically five orders of magnitude smaller.

Suspension Lines

The suspension system is simplified to rods from the ends of each load patch to the confluence point. The suspension lines, Fig. 2, are considered as three springs in series: a single $\frac{3}{8}$ -in.-diam rope, a double $\frac{3}{8}$ rope, and four $5/32$ wire ropes. The equivalent elastic modulus times area, EA , is found by

$$\frac{L}{EA} = \frac{L_1}{(EA)_1} + \frac{L_2}{(EA)_2} + \frac{L_3}{(EA)_3} \quad (4)$$

where L is the total length of the assembly. Using the actual lengths and elastic properties this becomes

$$\frac{L}{EA} = \frac{L-20}{23,200} + \frac{10}{2(23,200)} + \frac{10}{4(21,400)} \quad (5)$$

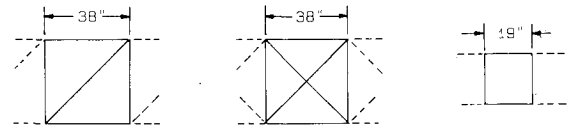


Fig. 3 Fin rib configuration.

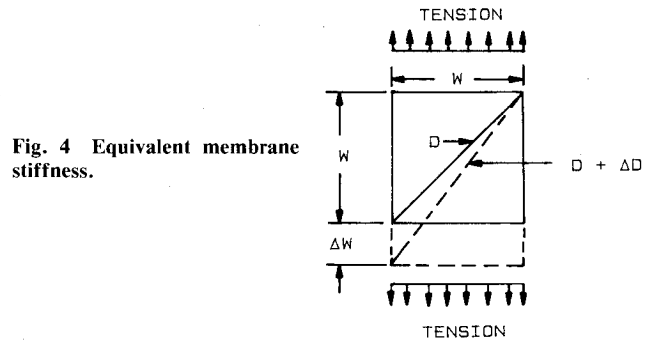


Fig. 4 Equivalent membrane stiffness.

Fin Ribs

The internal ribs of the fins consist of scallops and lacing. These are in three different configurations, as shown in Fig. 3: no diagonals, single diagonal, or double diagonal.

Assuming square segments, the equivalent membrane stiffness may be found by considering the force required to deflect the segment by ΔW (see Fig. 4).

$$F = (ET)_N W$$

$$= \frac{\Delta W}{W} (EA)_L + \frac{\Delta D}{D} (EA)_L \left(\frac{1}{\sqrt{2}} \right) N \quad (6)$$

where

$$D = W\sqrt{2} \quad (7)$$

and

$$\Delta D = W/\sqrt{2} \quad (8)$$

Substituting Eqs. (7) and (8) into Eq. (6) and solving for $(ET)_N$,

$$(ET)_N = \frac{(EA)_L}{W} \left(1 + \frac{N}{2\sqrt{2}} \right) \quad (9)$$

In a similar manner, the equivalent shear modulus times thickness, GT , is

$$(GT)_N = \frac{(EA)_L}{W} \left(\frac{N}{2\sqrt{2}} \right) \quad (10)$$

The actual ET 's and GT 's are found using an $(EA)_L$ of the lacing cord of 2800 lb and the lengths shown in Fig. 3. The densities are found by dividing the weight of a typical rib by its area.

Material Properties Summary

A summary of all material properties used in the analysis is given in Table 1. The same values were used for both the 250 and 365 aerostats.

Loading Conditions

The applied forces include internal pressure, buoyancy, gravity, and aerodynamic loads. Individual load cases are first used to check the accuracy of the model and of the load input. Then combinations of the loads are used to simulate actual loading conditions.

Table 1 Material properties

Description	Elastic modulus, psf	Shear modulus, psf	Density, pcf
Hull and fin—membrane	— ^a	— ^a	0.055
Hull and fin—bending	500	500	
Hull with ballonnet weight			0.105
Hull with ballonnet end cap weight			0.115
Suspension line 1	15,800		0.20
Suspension line 2	16,400		0.28
Suspension line 3	16,600		0.28
Suspension line 4	16,400		0.28
Suspension line 5	15,600		0.28
Suspension line 6	15,000		0.20
Suspension line 7	14,300		0.18
Fin rib—0 diag	1,800	0	0.059
Fin rib—1 diag	1,200	310	0.032
Fin rib—2 diag	1,500	620	0.052
Fin guy line	88,000		
Load patch	2,500		
T tape	2,000		
X tape	2,700		

^a Anisotropic material, see Eq. (3).

Internal Pressure

Internal pressure is a constant pressure applied to each two-dimensional element of the hull, fin side wall, and fin tip. The internal pressure used is normally 2.0 in. of water plus 80% of the dynamic pressure of the wind: 4.6 in. of water at 70 knots at sea level and 6.3 in. of water at 90 knots. Some cases were run at a low pressure (0.5 in. of water) to check for the possibility of hull buckling.

Buoyancy

Buoyancy or lift is the displaced volume times the specific lift. To incorporate this load properly, a pressure load is applied to each element which is proportional to the distance Z from an arbitrary reference point Z_0 (see Fig. 5).

The pressure P on any element due to buoyancy is

$$P = P_H - P_A = (Z_0 - Z)(\rho_A - \rho_H) \quad (11)$$

where P_H is the pressure of the helium, P_A is the pressure of the air, ρ_A is the density of air, and ρ_H is the density of helium.

For standard conditions at sea level the specific lift is $\rho_A - \rho_H = 0.06592 \text{ lb/ft}^3$.

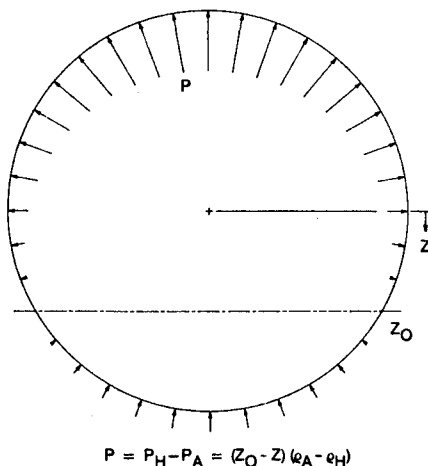


Fig. 5 Buoyancy load distribution.

For other flight altitudes the density ρ as a factor of the density at sea level ρ_0 and altitude H is

$$\rho = \rho_0 \left[\frac{T_0 - AH}{T_0} \right]^{4.2558} \quad (12)$$

where T_0 is the standard temperature of 518.67 R, and A is the standard lapse rate of 0.00356616 deg/ft. From this the specific lift is 0.04868 at 10,000 ft.

The reference point selected was the location of the helium pressure sensor at the bottom of the hull. Note that the pressure at the top of the hull will be about 0.5 in. of water higher than at the reference point.

Gravity

The mass of the structure is computed from the density of the elements. A gravitational acceleration and forces at the payload location are applied to obtain the desired system weight.

The model is free to pivot about the confluence point. An inertial load is automatically applied to balance all other moments about the confluence point.

Aerodynamic

Aerodynamic pressure distribution data is available from wind-tunnel tests.² The pressure data was interpolated between pressure taps to determine the C_p (pressure coefficient) for each element on the analysis model. The pressure on any element is then computed by QC_p , where Q is the dynamic pressure of the wind. Figure 6 is a typical pressure distribution map of the 365 aerostat hull with an angle of attack of 6 deg.

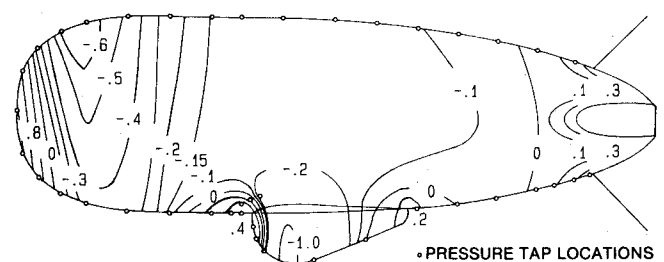


Fig. 6 Pressure distribution map.

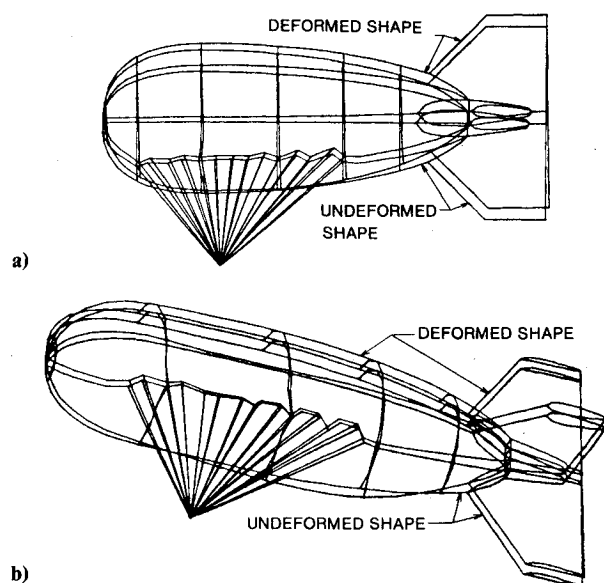


Fig. 7 Static deformations, 70-knot winds: a) 250 aerostat; b) 365 aerostat.

Combined Loads

Combinations of the above loads are used to simulate actual flying conditions. Dynamic pressures of 0, 16.6, and 27.7 lb/ft² were used representing winds of 0, 70, and 90 knots at sea level. The angle of attack was 6 deg. The corresponding internal pressures were 2.0, 4.5, and 6.3 in. of water. The specific lifts used were 0.04868 lb/ft³ for the 365 aerostat and 0.04358 for the 250 aerostat corresponding to standard day altitudes of 10,000 and 18,000 ft. This gives buoyant lifts of 18,400 and 11,800 lb. The gravitational acceleration of 1g down was used.

Other combinations used included a lower internal pressure (0.5 in. of water) with no wind to check for hull buckling. Winds at an angle of attack of 20 deg were used to simulate a gusting wind.

Results

Shape

With an internal pressure load of 2 in. of water, the length of the aerostat increases by 3% and the diameter by 7%. The buoyancy load causes the hull cross section to become elliptical with the height greater than the width—especially in the cylindrical section of the 365 aerostat.

Figures 7a and 7b are plots of the deformed shape superimposed over the undeformed shape with a 70-knot wind loading. Notice that the suspension lines stretch causing the entire aerostat to deflect upward. The aft hull deflects upward because of the lift of the helium in the fins. The bottom of the hull deflects downward because of the weight of the payload. The elliptical shape of the hull can be seen in Fig. 7b. These deformations are exaggerated in the plots so that they may be easily seen.

The volume V of the aerostat can be found by

$$V = F_z / \lambda \quad (13)$$

Table 2 Computed geometric parameters

	250 aerostat	365 aerostat
Hull volume, ft ³	242,850	356,874
Hull center of volume, ft	62.2	83.5
Empennage volume, ft ³	30,523	24,738
Empennage center of volume, ft	152.5	181.5

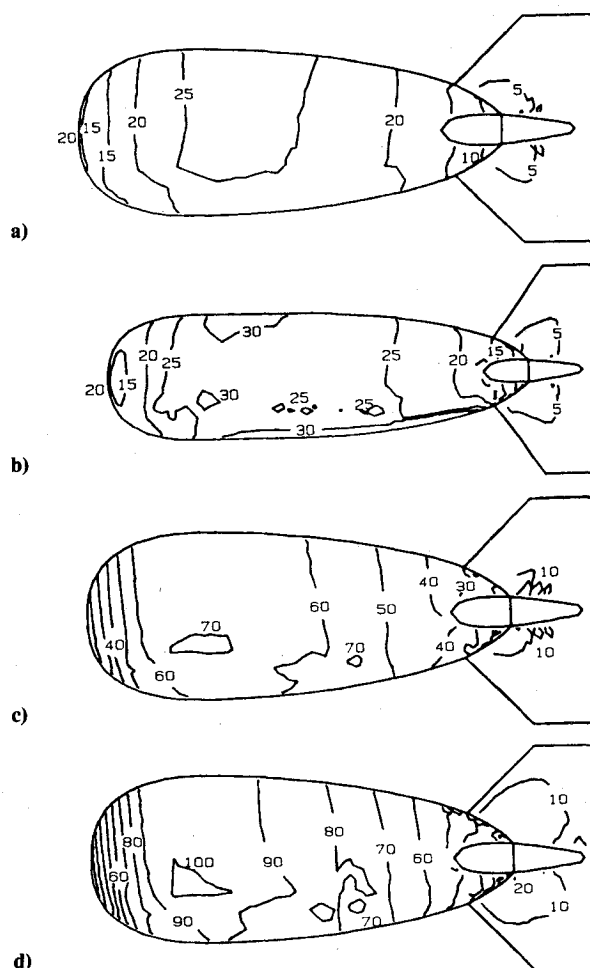


Fig. 8 Major principal stresses: a) 250 aerostat, no wind; b) 365 aerostat, no wind; c) 250 aerostat, 70-knot wind; d) 250 aerostat, 90-knot wind.

where F_z is the vertical reactive force and λ is the specific lift used. The center of volume \bar{x} can be found by

$$F_z \bar{x} = F_x D \quad (14)$$

where F_x is the longitudinal reactive force and D is the distance from the reaction to the confluence point about which moments are added. This results in the volumes and centroids found in Table 2.

Note that these undeformed volumes are slightly smaller than the theoretical volumes. This is because the finite elements of the model form secants with the theoretical shape. The 365 empennage volume is for three fins only.

Maximum Stresses

With an internal pressure load only, the hoop stress σ_H and meridional stress σ_M at the maximum diameter are close to the stresses found by

$$\sigma_H = PR \quad \text{and} \quad \sigma_M = \frac{1}{2}PR \quad (15)$$

where P is the internal pressure and R is the radius. The maximum stress occurs at the point of maximum diameter; the next highest stress is at the nose. The nose is nearly flat but tries to become spherical with pressure load.

Figures 8a-d are contour plots of major principal (maximum) stresses with combined loads. Note that the highest stresses occur in the area of maximum diameter. The stresses here are higher above suspension line load patches and lower below the patches. The stresses in the fins and aft hull are much lower.

Table 3 Summary of results

Aerostat	Wind/angle, knot/deg	Internal pressure, in H ₂ O	Tether tension, lb	Suspension line tension, lb	Fin guy tension, lb	Hull stress, lb/in.	Fin stress, lb/in.	Fin rib stress, lb/in.
250	0	2.0	4,800	670	10	28	15	4
	70/6	4.6	11,400	1,200	520	71	32	9
	90/6	6.3	15,900	1,840	860	101	43	12
	0	0.5	4,800	660	0	13	6	1
365	0	2.0	7,500	1,300	60	33	17	3
	70/6	4.5	21,500	2,500	500	77	32	9
	90/6	6.3	31,000	3,500	820	106	43	12
	0	0.5	7,500	1,300	80	14	8	1
	70/20	4.6	31,100	3,100	1,250	77	40	9
	90/20	6.3	45,100	4,700	2,080	107	57	13
Allowable				9,600	5,600	150 225	150 225	45

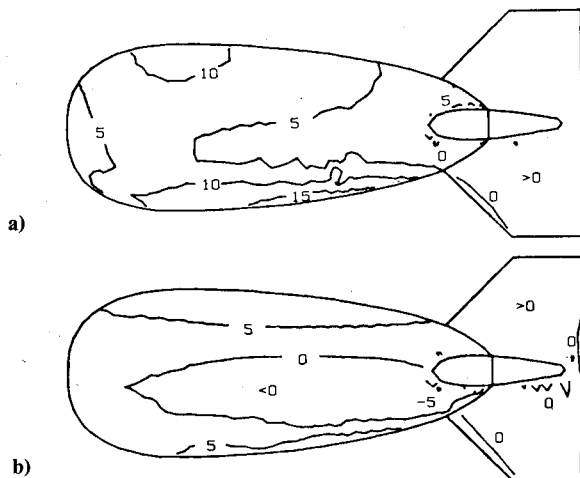
**Fig. 9** Minor principal stresses: a) normal pressure, 70-knot wind; b) low pressure, no wind.**Buckling**

Figure 9a is a plot of minor principal (minimum) stresses under normal loading conditions. There are no indications of hull buckling as would be shown by negative (compressive) stresses. With a low internal pressure, Fig. 9b, an extensive area of the hull shows negative stresses.

Suspension System

The suspension lines stretch enough to have a nearly uniform loading. The average suspension system spring constant is 4000 lb/ft. This is found by

$$K = F_z / U_z \quad (16)$$

where F_z is the confluence point tension and U_z is the average vertical displacement of the aerostat with the load.

Summary

A summary of results for representative load cases is shown in Table 3. The allowable stress for the hull material is 150 lb/in. for a long term static load or 225 lb/in. for dynamic loads. The safety factors for the conservative load of a 90-knot wind at 6 deg are found in Table 4.

The hull and fin stresses are nearly the same on a 250 aerostat as on a 365: these stresses are primarily a function of

Table 4 Safety factors

	250 aerostat	365 aerostat
Hull material	1.5	1.4
Fin material	3.5	3.5
Fin rib	3.8	3.8
Fin guy line	6.5	6.8
Suspension line	5.2	2.7

internal pressure and maximum diameter, which are the same on both. The tether tension and suspension line tension are higher on a 365 because of increased net lift and aerodynamic forces.

Conclusions

The analysis of the 250 and 365 aerostats show all stresses to be less than the allowable for the design loading conditions. There are no indications of buckling at the design operating conditions.

The hull material safety factor is 1.5 for 90-knot, long-term load or 2.2 for short-term load. The stresses are evenly distributed with the highest stresses, depending on the loading conditions, being in the areas of the maximum diameter, the nose, the load patches, and the payload attachment. The use of different materials in various areas of the hull would not be practical.

The safety factors on the fin side walls, fin ribs, and fin guy lines are high. In order to optimize the materials for weight reduction, lighter materials could be used here.

The overall stress patterns and deformations of aerostats can be analyzed by the finite-element method. The results agree with other methods of analysis when this can be done. Shape measurements made under the zero wind case show the same trend as the analysis.

This finite-element analysis is based on small deflection theory. More accuracy could be obtained by considering large strains and large angular deformations. This could be done in localized areas only of the aerostat in order to reduce computer costs.

References

- ¹Lagerquist, D.R., "G1428 Hull Laminate Biaxial Stress Cylinder Tests Stiffness Matrix Calculation," Sheldahl Inc., Northfield, Minn., July 1979.
- ²Gove, T.B. and Haak, E.L., "MK VII and MK VII-S Wind Tunnel Study," Sheldahl Inc., Northfield, Minn., SER 0185, May 1974.